Journal of Sound and Vibration 328 (2009) 575–585

Contents lists available at ScienceDirect

Journal of Sound and Vibration

journal homepage: www.elsevier.com/locate/jsvi

Transmission loss estimation of three-dimensional silencers by system graph approach using multi-domain BEM

Young-Bum Park [a,b,c], Hyeon-Don Ju [a,b,c,*], Shi-Bok Lee [a,b,c]

[a] DK Industrial Co., Ltd., 511, Sinpyeong-Dong, Saha-Gu, Pusan 604-030, Korea
[b] Department of Fire & Disaster Prevention Engineering, Korea International University, Chinju 660-759, Korea
[c] School of Mechanical Engineering, Pusan National University, Pusan 609-735, Korea

ARTICLE INFO

Article history:
Received 14 December 2007
Received in revised form
11 August 2009
Accepted 21 August 2009
Handling Editor: J. Lam
Available online 8 October 2009

ABSTRACT

Transmission loss (TL) estimation of three-dimensional silencers with complicated internal structures such as inlet/outlet tubes, thin baffles, perforated tubes, and sound absorbing materials is a demanding job even by powerful numerical approach such as FEM (finite element method) or BEM (boundary element method).

The transfer matrix method using the multi-domain BEM data may be an efficient tool to deal with multi-branched acoustic systems but the method has limitation in application since it is based on the assumption of plane wave propagation at the interface of sub-domains. Assembling the whole system equation directly using the multi-domain BEM data is a considerable means to deal with three-dimensional acoustic components, but the intermediate pseudo-unknown variables in the equation assembling process may be too large.

An efficient practical method by system graph approach and multi-domain BEM is proposed to formulate the condensed overall acoustic system equation for the whole acoustic system, only with unknown sound pressures on the sub-domain boundaries. The solutions of the overall equation are used to compute the TL of silencers.

An air suction silencer for air compressors is tested numerically and experimentally and both results are compared to back up the suggested method.

1. Introduction

In recent decades, intake and exhaust parts have been recognized as the primary noise sources in internal combustion machinery and industrial facilities. Silencers with very complicated internal acoustic components such as inlet/outlet tubes, thin baffles, perforated tubes, and sound absorbing materials have been introduced in automobiles, industrial equipments and environmental facilities [1,2]. The complex internal components of silencers would be adopted so as to improve the silencing efficiency, but introduce much difficulty in the analysis and design of the silencer. Air suction silencers installed in air compressors may be a typical example. The airborne noise generated in the compressor propagates through such components of the silencers and radiates into the atmosphere.

The finite element method(FEM), boundary element method (BEM), acoustic filter and transfer matrix method [3], transfer matrix method with BEM [4], multi-domain BEM [5], BEM combining the impedance matrices for any two

* Corresponding author at: Department of Fire & Disaster Prevention Engineering, International University of Korea, Chinju 660-759, Korea. Tel.: +82 55 751 8217; fax: +82 55 751 8210.
E-mail address: hdju2433@hanmail.net (H.-D. Ju).

0022-460X/$ - see front matter © 2009 Elsevier Ltd. All rights reserved.
doi:10.1016/j.jsv.2009.08.031

sub-domains in cascaded connection [6] and multi-domain structural-acoustic coupling analysis [7] have been applied to the analysis and design of complicated acoustic systems.

The transfer matrix method using the multi-domain BEM may be an efficient tool to deal with multi-branched acoustic systems. The overall transfer matrix of the whole acoustic system can be obtained by assembling all the transfer matrices of the sub-domains [4]. The method has limitation in application since it is based on the assumption of plane wave propagation at the interface of sub-domains, which is only true below the cutoff frequency. The overall transfer matrix of the silencer is calculated through serial multiplication of the sub-domain transfer matrices. When the silencers with three-dimensional complicated components, e.g., one with perforated tubes, are divided into several domains for the BEM analysis, plane wave propagations in the inlet and outlet boundaries of each sub-domain cannot be assumed anymore.

The direct BEM technique [8] and multi-domain BEM technique [5] were shown to be successful in determining the acoustic response and TL of the silencers with complicated components. A direct mixed-body BEM [9] was introduced to analyze mufflers with perforated tubes and produces a hyper-singular integral and many variables in the sub-domains. An impedance matrix synthesis method using the direct mixed-body BEM [10] was proposed to obtain the complete impedance matrix for each subsystem separately by many different BEM runs. Also, a sub-structuring technique combining the impedance matrices for assembling sub-structures using the direct mixed-body BEM was proposed [11]. The overall impedance matrix for TL estimation was adopted by connecting the impedance matrices of sub-domains [12]. The substructure BEM was employed to predict the transmission loss of a hybrid silencer [13].

We previously proposed a practical means, based on multi-domain BEM data, to formulate overall compact acoustic system equations which take only the particle velocities on the sub-domain interface boundaries as unknowns, the solutions of which are used to compute the overall transfer matrix elements [14]. But it still has somewhat complexity and limitation in dealing with complicated silencers systematically.

This paper investigates a new method to formulate the compact acoustic system equation for the whole acoustic system, condensed only for unknown sound pressures, excluding the particle velocity unknowns, on the sub-domain boundaries. In the assembling process of acoustic equations for the sub-domains, system graph approach [15] is utilized to deal with the complex acoustic system systematically and efficiently. The solution of the overall equation is used later to compute the TL of the silencing equipments.

To explain and validate the suggesting method for the TL determination, an air suction silencer divided into four sub-domains is tested experimentally and numerically and both results are compared. Air filters for air compressors have also the noise reduction role. That is the reason why the air filter of the compressor is considered as the air suction silencer. The air suction silencer considered in our paper is made up of a short inlet pipe, an expansion chamber filled with two perforated air filter guide pipes, and a relatively long outlet pipe.

2. Admittance matrix computation with multi-domain BEM

Consider a general multi-domain acoustic problem as shown in Fig. 1. It represents an acoustic body with the domain Ω enclosed by a boundary surface S, which can be divided into a few sub-domains separated by imaginary interfaces. Considering a three-dimensional enclosed acoustic cavity Ω consisting of the sub-domains, $\Omega_{\mathrm{I}}, \Omega_{\mathrm{II}}, \ldots, \Omega_i, \Omega_{i+1}, \ldots, \Omega_{N-1}, \Omega_N$, we apply the boundary integral formulation to each sub-domain. At the interfaces between the sub-domains, acoustic pressure equilibrium and compatibility of particle velocities should be satisfied. The sub-domain Ω_{I} is enclosed by the inherent boundary S_1^{I} and new interface boundary S_2^{I}. Similarly the inherent boundary S_2^{II}, boundary $S_1^{\mathrm{II}}(S_2^{\mathrm{I}})$ interfacing Ω_{I} and new boundary S_3^{II} interfacing the sub-domain Ω_{III} encapsulate the sub-domain Ω_{II}.

For the i-th sub-domain Ω_i, a boundary integral equation may be written as Eq. (1). The medium in Ω_i is assumed as a compressible, in-viscid and non-flowing fluid. For the time-harmonic excitation, the velocity potential Φ in the fluid satisfies the Kirchhoff–Helmholtz equation [16]:

$$C^0(P)\Phi(P) = \int_S \left[\psi(P,Q)\frac{\partial \Phi}{\partial n}(Q) - \Phi(Q)\frac{\partial \Psi}{\partial n}(P,Q)\right] \mathrm{d}S(Q) \tag{1}$$

where P is a collocation point, Q is any integration point on the boundary S and n denotes the coordinate normal to the surface. The function Ψ is the three-dimensional free-domain Green's function, $\psi(P,Q) = \exp[\mathrm{i}kR(P,Q)]/R(P,Q)$ in which $R(P,Q)$ is the distance between P and Q and k is the wavenumber.

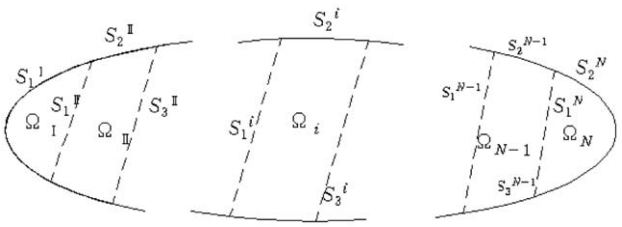

Fig. 1. Acoustic structure divided into sub-domains.

The coefficient $C^0(P)$ has the value of 4π for P in any domain and on any arbitrary surface can be evaluated by the following equation:

$$C^0(P) = -\int_S \frac{\partial}{\partial n}\left(\frac{1}{R(P,Q)}\right) \mathrm{d}S(Q) \tag{2}$$

By dividing the boundary surface (including the interfaces) into a number of elements, the boundary integral equation can be transformed into algebraic simultaneous equations as follows:

$$\sum_{l=1}^{M} B_{jl} \cdot p_l = \sum_{l}^{M} A_{jl} \cdot u_l \quad (j = 1, 2, \ldots, M) \tag{3a}$$

or

$$[B]\{p\} = [A]\{u\} \tag{3b}$$

where M represents the number of collocation points(the number of nodes on the boundary surface), l denotes the l-th collocation point, j denotes the j-th node on the boundary and $\{p\}$ and $\{u\}$ represent sound pressure and particle velocity vector, respectively.

Here, Eq. (3b) is rewritten as

$$\{u\} = [G]\{p\} \tag{4}$$

where $[G] = [A]^{-1}[B]$ is the admittance matrix and $[A]^{-1}$ means the inverse matrix of $[A]$.

Also, Eq. (3b) is rewritten as

$$\{p\} = [D]\{u\} \tag{5}$$

where $\{D\} = [B]^{-1}[A]$ is the impedance matrix.

3. Overall system equation and transmission loss

3.1. Overall system equation by system graph approach

As shown in Figs. 2, 3 and 4, an air suction silencer was adopted as an acoustic model to explain the proposing method.

Here, we derive an overall acoustic system equation for the unknown sound pressures on the sub-domain boundaries. The input constants in the equation are the particle velocities at the domain boundaries and the coefficient matrix is overall admittance matrix. Finally, the sound pressure solutions at the inlet and outlet boundaries will be used to compute the transmission loss.

The overall system equation is assembled from all the acoustic equations governing sub-domains formulated by Eq. (4). This assembling process for complex acoustic systems with complicatedly connected sub-domains is a very confusing and demanding work. To treat this problem systematically and efficiently, we rely on system graph approach, which is a universal tool used in diverse system dynamics modeling.

Taking into the consideration of the acoustic contribution of the perforated guide pipes, we divide the three-dimensional silencer system into four domains, Ω_{I}, Ω_{II}, Ω_{III} and Ω_{IV} as shown in Fig. 5. Ω_{I} and Ω_{IV} are the intake and outtake sub-domain, respectively. Ω_{II} and Ω_{III} represent the intermediate sub-domains divided by two perforated guide pipes, respectively. The sub-domain Ω_{II} is the space for the air filter to be inserted into.

We express the particle velocities crossing through the boundary n into or from Ω_K as $\{u_n^K\}$ and the sound pressures at the boundary n of the sub-domain Ω_K as $\{p_n^K\}$, in which the boundary numbers of 1, 2,…, 8 and 9 are used for the

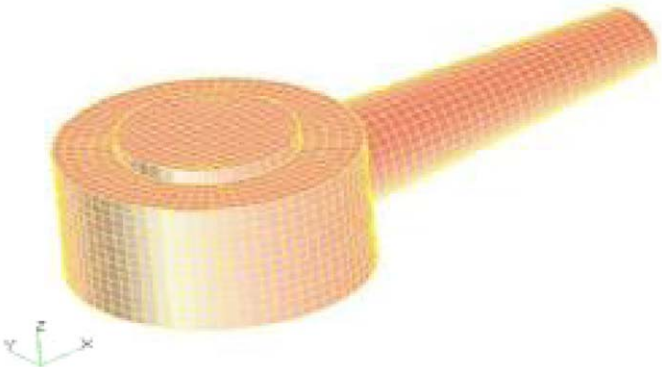

Fig. 2. Boundary element model of the air suction silencer.

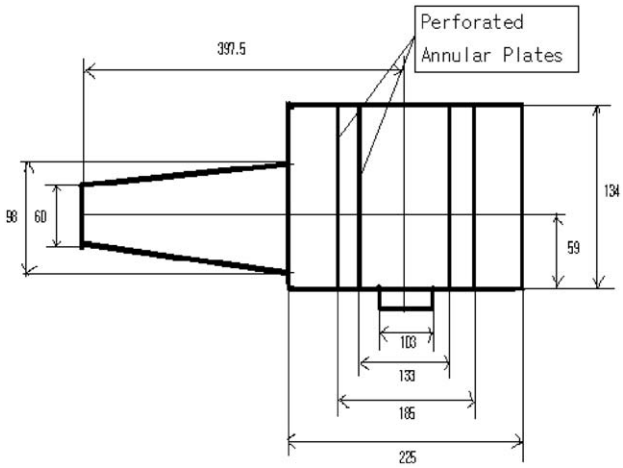

Fig. 3. Dimensions of the air suction silencer with internal perforated pipes.

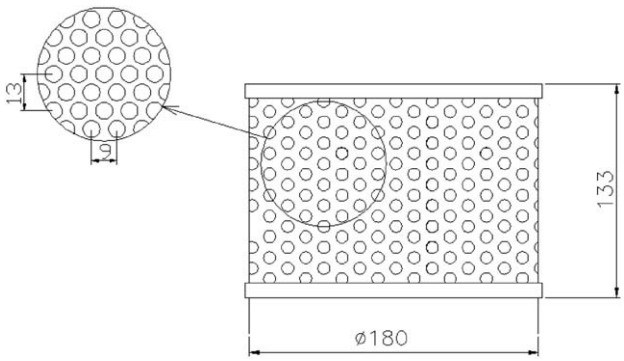

Fig. 4. Schematic of the perforated pipes.

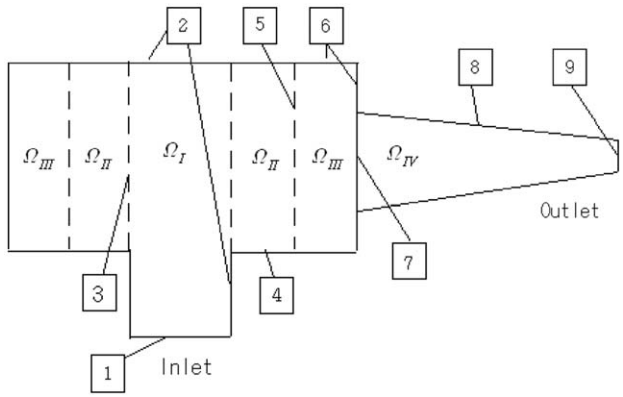

Fig. 5. Four sub-domains of the air suction silencer with internal perforated pipes.

subscript n and the sub-domain numbers of I, II, III and IV for the superscript K. For example, incoming particle velocities through the inlet boundary 1 into Ω_{I} are represented as $\{u_1^{\mathrm{I}}\}$ and outgoing particle velocities through the outlet boundary 9 from Ω_{IV} as $\{u_9^{\mathrm{IV}}\}$.

To reduce the equation variables, we use the self-evident relations between the acoustic variables, i.e. sound pressures and air particle velocities. By the compatibility of particle velocities, the particle velocities at the interface boundaries between sub-domains are related as follows:

$$\{u_3^{\mathrm{II}}\} = -\{u_3^{\mathrm{I}}\} \tag{8}$$

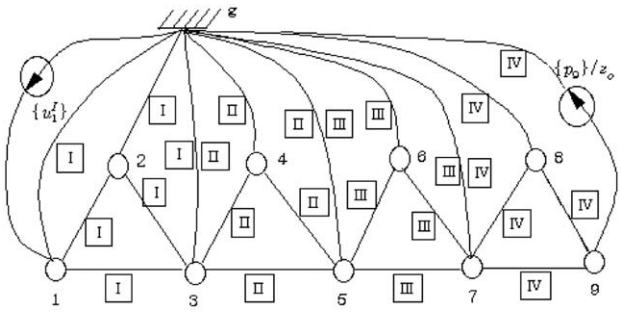

Fig. 6. System graph of the air suction silencer.

$$\{u_5^{II}\} = -\{u_5^{III}\} \tag{9}$$

$$\{u_7^{III}\} = -\{u_7^{IV}\} \tag{10}$$

Using the impedance matrices of the interface boundaries between the sub-domains, the sound pressure differences across the interface boundaries can be related as follows:

$$\{p_3^{II}\} = \{p_3^{I}\} + [Z_{I\,II}]\{u_3^{II}\} \tag{11}$$

$$\{p_5^{III}\} = \{p_5^{II}\} + [Z_{II\,III}]\{u_5^{III}\} \tag{12}$$

where $[Z_{I\,II}]$ and $[Z_{II\,III}]$ denote the impedance matrix between Ω_I and Ω_{II} and between Ω_{II} and Ω_{III}, respectively. Sound pressure equilibrium at the boundary 7 between the sub-domain III and IV gives

$$\{p_7^{III}\} = \{p_7^{IV}\}$$

Here, for the convenience of expression, the sound pressure symbols are re-expressed as $\{p_1^I\} \equiv \{p_1\}$, $\{p_2^I\} \equiv \{p_2\}$, $\{p_3^I\} \equiv \{p_3\}$, $\{p_4^{II}\} \equiv \{p_4\}$, $\{p_5^{II}\} \equiv \{p_5\}$, $\{p_6^{III}\} \equiv \{p_6\}$, $\{p_7^{III}\} = \{p_7^{IV}\} \equiv \{p_7\}$, $\{p_8^{IV}\} \equiv \{p_8\}$, $\{p_9^{IV}\} \equiv \{p_9\}$.

Acoustic connection structure between the sub-domains in Fig. 5 is expressed as a system graph as shown in Fig. 6 for a systematic and efficient assembling process of the overall system equation. z_0 is the characteristic impedance of the anechoic termination and $\{p_9\}/z_0$ is the particle velocity vector $\{u_9^{IV}\}$ at the outlet boundary 9.

The sub-domain can be represented as a four-terminal component model in the system graph and so should be described by three system equations. For the sub-domain Ω_I, Eq. (4) is expressed as follows:

$$\begin{bmatrix} \{u_1^I\} \\ \{u_2^I\} \\ \{u_3^I\} \end{bmatrix} = \begin{bmatrix} [G_{1,1}^I] & [G_{1,2}^I] & [G_{1,3}^I] \\ [G_{2,1}^I] & [G_{2,2}^I] & [G_{2,3}^I] \\ [G_{3,1}^I] & [G_{3,2}^I] & [G_{3,3}^I] \end{bmatrix} \begin{bmatrix} \{p_1\} \\ \{p_2\} \\ \{p_3\} \end{bmatrix} \tag{13}$$

Similarly, Eq. (5) writes for the sub-domain Ω_{II} as follows:

$$\begin{bmatrix} \{p_3^{II}\} \\ \{p_4^{II}\} \\ \{p_5^{II}\} \end{bmatrix} = \begin{bmatrix} [D_{3,3}^{II}] & [D_{3,4}^{II}] & [D_{3,5}^{II}] \\ [D_{4,3}^{II}] & [D_{4,4}^{II}] & [D_{4,5}^{II}] \\ [D_{5,3}^{II}] & [D_{5,4}^{II}] & [D_{5,5}^{II}] \end{bmatrix} \begin{bmatrix} \{u_3^{II}\} \\ \{u_4^{II}\} \\ \{u_5^{II}\} \end{bmatrix} \tag{14}$$

Using Eq. (11), Eq. (14) can be rewritten as follows:

$$\begin{bmatrix} \{u_3^{II}\} \\ \{u_4^{II}\} \\ \{u_5^{II}\} \end{bmatrix} = \begin{bmatrix} [G_{3,3}^{II}] & [G_{3,4}^{II}] & [G_{3,5}^{II}] \\ [G_{4,3}^{II}] & [G_{4,4}^{II}] & [G_{4,5}^{II}] \\ [G_{5,3}^{II}] & [G_{5,4}^{II}] & [G_{5,5}^{II}] \end{bmatrix} \begin{bmatrix} \{p_3\} \\ \{p_4\} \\ \{p_5\} \end{bmatrix} \tag{15}$$

where

$$\begin{bmatrix} [G^{II}_{3,3}] & [G^{I}_{3,4}] & [G^{II}_{3,5}] \\ [G^{II}_{4,3}] & [G^{II}_{4,4}] & [G^{II}_{4,5}] \\ [G^{II}_{5,3}] & [G^{II}_{5,4}] & [G^{II}_{5,5}] \end{bmatrix} = \begin{bmatrix} [D^{II}_{3,3} - Z_{I\,II}] & [D^{II}_{3,4}] & [D^{II}_{3,5}] \\ [D^{II}_{4,3}] & [D^{II}_{4,4}] & [D^{II}_{4,5}] \\ [D^{II}_{5,3}] & [D^{II}_{5,4}] & [D^{II}_{5,5}] \end{bmatrix}^{-1}$$

The sound pressures and particle velocities in Eq. (15) are unknowns.

By treating the perforated guide pipes as impedance elements, the sound pressure equilibrium condition on the sub-domain boundaries with perforations can be easily implemented [5]. For low air velocities through the perforate holes on the interface boundary, the transfer impedance can be calculated by

$$Z = \rho_o c_o [0.006 + ik(t_w + 0.75 d_h)]/\phi \tag{16}$$

where $\rho_o c_o$ depicts the characteristic impedance of the air, i the imaginary number, t_w the thickness of the perforated pipe, d_h the perforate hole diameter and ϕ the porosity [17].

Applying the same procedure to the sub-domain Ω_{III}, the similar equation for the particle velocities and pressures at the boundary of Ω_{III} is derived:

$$\begin{bmatrix} \{u^{III}_5\} \\ \{u^{III}_6\} \\ \{u^{III}_7\} \end{bmatrix} = \begin{bmatrix} [G^{III}_{5,5}] & [G^{III}_{5,6}] & [G^{III}_{5,7}] \\ [G^{III}_{6,5}] & [G^{III}_{6,6}] & [G^{III}_{6,7}] \\ [G^{III}_{7,5}] & [G^{III}_{7,6}] & [G^{III}_{7,7}] \end{bmatrix} \begin{bmatrix} \{p_5\} \\ \{p_6\} \\ \{p_7\} \end{bmatrix} \tag{17}$$

where

$$\begin{bmatrix} [G^{III}_{5,5}] & [G^{III}_{5,6}] & [G^{III}_{5,7}] \\ [G^{III}_{6,5}] & [G^{III}_{6,6}] & [G^{III}_{6,7}] \\ [G^{III}_{7,5}] & [G^{III}_{7,6}] & [G^{III}_{7,7}] \end{bmatrix} = \begin{bmatrix} [D^{III}_{5,5} - Z_{II\,III}] & [D^{III}_{5,6}] & [D^{III}_{5,7}] \\ [D^{III}_{6,5}] & [D^{III}_{6,6}] & [D^{III}_{6,7}] \\ [D^{III}_{7,5}] & [D^{III}_{7,6}] & [D^{III}_{7,7}] \end{bmatrix}^{-1}$$

Also, assuming anechoic termination at the outlet and applying the same procedure to the sub-domain Ω_{IV}, the similar equation for the particle velocities and pressures at the boundary of Ω_{IV} is derived as follows:

$$\begin{bmatrix} \{u^{IV}_7\} \\ \{u^{IV}_8\} \\ \{u^{IV}_9\} \end{bmatrix} = \begin{bmatrix} [G^{IV}_{7,7}] & [G^{IV}_{7,8}] \\ [G^{IV}_{8,7}] & [G^{IV}_{8,8}] \\ [G^{IV}_{9,7}] & [G^{IV}_{9,8}] \end{bmatrix} \begin{bmatrix} \{p_7\} \\ \{p_8\} \end{bmatrix} \tag{18}$$

where

$$\begin{bmatrix} [G^{IV}_{7,7}] & [G^{IV}_{7,8}] \\ [G^{IV}_{8,7}] & [G^{IV}_{8,8}] \\ [G^{IV}_{9,7}] & [G^{IV}_{9,8}] \end{bmatrix} = \begin{bmatrix} [A^{IV}_{7,7}] & [A^{IV}_{7,8}] & [A^{IV}_{7,9} - z_0 B^{IV}_{7,9}] \\ [A^{IV}_{8,7}] & [A^{IV}_{8,8}] & [A^{IV}_{8,9} - z_0 B^{IV}_{8,9}] \\ [A^{IV}_{9,7}] & [A^{IV}_{9,8}] & [A^{IV}_{9,9} - z_0 B^{IV}_{9,9}] \end{bmatrix}^{-1} \begin{bmatrix} [B^{IV}_{7,7}] & [B^{IV}_{7,8}] \\ [B^{IV}_{8,7}] & [B^{IV}_{8,8}] \\ [B^{IV}_{9,7}] & [B^{IV}_{9,8}] \end{bmatrix}$$

The terminal graphs for the sub-domain I in Fig. 6 are taken out in Fig. 7. With the four-terminal components, the sub-domain I can be described by the following three vertex system equations.

$$1.\quad [G^{I}_{1,1}]\{p_1\} + [G^{I}_{1,2}]\{p_2\} + [G^{I}_{1,3}]\{p_3\} + \{u^{I}_1\} = 0 \tag{19a}$$

$$2.\quad [G^{I}_{2,1}]\{p_1\} + [G^{I}_{2,2}]\{p_2\} + [G^{I}_{2,3}]\{p_3\} = 0 \tag{19b}$$

$$3.\quad [G^{I}_{3,1}]\{p_1\} + [G^{I}_{3,2}]\{p_2\} + ([G^{I}_{3,3}] + [G^{II}_{3,3}])\{p_3\} + [G^{II}_{3,4}]\{p_4\} + [G^{II}_{3,5}]\{p_5\} = 0 \tag{19c}$$

Similarly, all the rest vertices 4, 5, 6, 7, 8 and 9 in Fig. 6 are formulated respectively as follows:

$$4.\quad [G^{II}_{4,3}]\{p_3\} + [G^{II}_{4,4}]\{p_4\} + [G^{II}_{4,5}]\{p_5\} = 0 \tag{19d}$$

$$5.\quad [G^{II}_{5,3}]\{p_3\} + [G^{II}_{5,4}]\{p_4\} + ([G^{II}_{5,5}] + [G^{III}_{5,5}])\{p_5\} + [G^{III}_{5,6}]\{p_6\} + [G^{III}_{5,7}]\{p_7\} = 0 \tag{19e}$$

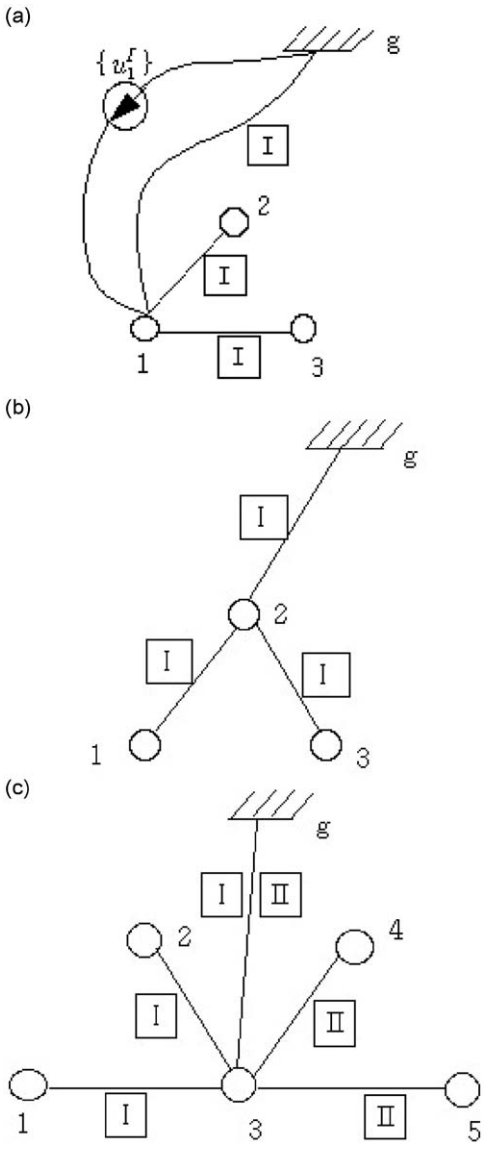

Fig. 7. Terminal graph of the sub-domain: (a) node 1, (b) node 2, and (c) node 3.

$$6.\quad [G^{III}_{6,5}]\{p_5\} + [G^{III}_{6,6}]\{p_6\} + [G^{III}_{6,7}]\{p_7\} = 0 \tag{19f}$$

$$7.\quad [G^{III}_{7,5}]\{p_5\} + [G^{III}_{7,6}]\{p_6\} + ([G^{III}_{7,7}] + [G^{IV}_{7,7}])\{p_7\} + [G^{IV}_{7,8}]\{p_8\} = 0 \tag{19g}$$

$$8.\quad [G^{IV}_{8,7}]\{p_7\} + [G^{IV}_{8,8}]\{p_8\} = 0 \tag{19h}$$

$$9.\quad \{p_9\}/z_0 = \{u^{IV}_9\} = [G^{IV}_{9,7}]\{p_7\} + [G^{IV}_{9,8}]\{p_8\} \tag{19i}$$

Eqs. (19a)–(19h) are assembled as an overall system equation as follows:

$$[A]\cdot\{p\} = \{B\} \tag{20}$$

where $\{p\}^{\mathrm{T}} = \{\{p_1\}^{\mathrm{T}}, \{p_2\}^{\mathrm{T}}, \{p_3\}^{\mathrm{T}}, \{p_4\}^{\mathrm{T}}, \{p_5\}^{\mathrm{T}}, \{p_6\}^{\mathrm{T}}, \{p_7\}^{\mathrm{T}}, \{p_8\}^{\mathrm{T}}\}$, $\{B\}^{\mathrm{T}} = \{\{u_1^{\mathrm{I}}\}^{\mathrm{T}}, \{0\}, \{0\}, \{0\}, \{0\}, \{0\}, \{0\}, \{0\}\}$, and the node admittance matrix $[A]$ is

$$\begin{vmatrix}
[G^{\mathrm{I}}_{1,1}] & [G^{\mathrm{I}}_{1,2}] & [G^{\mathrm{I}}_{1,3}] & [0] & [0] & [0] & [0] & [0] \\
[G^{\mathrm{I}}_{2,1}] & [G^{\mathrm{I}}_{2,2}] & [G^{\mathrm{I}}_{2,3}] & [0] & [0] & [0] & [0] & [0] \\
[G^{\mathrm{I}}_{3,1}] & [G^{\mathrm{I}}_{3,2}] & [G^{\mathrm{I}}_{3,3}] + [G^{\mathrm{II}}_{3,3}] & [G^{\mathrm{II}}_{3,4}] & [G^{\mathrm{II}}_{3,5}] & [0] & [0] & [0] \\
[0] & [0] & [G^{\mathrm{II}}_{4,3}] & [G^{\mathrm{II}}_{4,4}] & [G^{\mathrm{II}}_{4,5}] & [0] & [0] & [0] \\
[0] & [0] & [G^{\mathrm{II}}_{5,3}] & [G^{\mathrm{II}}_{5,4}] & [G^{\mathrm{II}}_{5,5}] + [G^{\mathrm{III}}_{5,5}] & [G^{\mathrm{III}}_{5,6}] & [G^{\mathrm{III}}_{5,7}] & [0] \\
[0] & [0] & [0] & [0] & [G^{\mathrm{III}}_{6,5}] & [G^{\mathrm{III}}_{6,6}] & [G^{\mathrm{III}}_{6,7}] & [0] \\
[0] & [0] & [0] & [0] & [G^{\mathrm{III}}_{7,5}] & [G^{\mathrm{III}}_{7,6}] & [G^{\mathrm{III}}_{7,7}] + [G^{IV}_{7,7}] & [G^{\mathrm{IV}}_{7,8}] \\
[0] & [0] & [0] & [0] & [0] & [0] & [G^{\mathrm{IV}}_{8,7}] & [G^{\mathrm{IV}}_{8,8}]
\end{vmatrix}$$

3.2. Transmission loss estimation

TL is derived as the ratio of the power incident on the silencer to the power transmitted through the silencer and can be expressed as follows [3]:

$$TL = -10\log_{10}\left(\left|\frac{p_9}{p_1^+}\right|^2 \frac{S_9}{S_1}\right) \tag{21}$$

where p_1^+ and p_9 are the incident sound pressure at the inlet boundary and the sound pressure at the outlet boundary, respectively, S_1 and S_9 are the cross-sectional areas of the inlet and outlet of the silencer, respectively.

The sound pressure and sound particle velocity at the inlet boundary of the silencer can be expressed, respectively, as follows:

$$p_1 = p_1^+ + p_1^- \tag{22}$$

$$u_1 = \frac{1}{z_0}(p_1^+ + p_1^-) \tag{23}$$

where p_1^- is the reflected sound pressure at the inlet boundary, respectively.

By Eqs. (22) and (23), the incident sound pressure at the inlet boundary is expressed as follows:

$$p_1^+ = 0.5(p_1 + z_0 u_1) \tag{24}$$

Now, we require only p_1 and p_9 to compute the transmission loss, which is the solutions of the system equations (20) and (19i).

4. Experiments and discussion

4.1. Experimental apparatus and procedure

Fig. 8 shows the schematic diagram of the experimental setup for transmission loss measurement of the air suction silencer. TL of the air suction silencer is measured by the two-microphone method [18]. A signal generator produces the specified random-noise signal, which is passed through a power-amplifier before it is fed to a horn driver, to excite the acoustic field. The signal picked up by each microphone (B&K type 4188) is amplified by a conditioning amplifier, and then goes to the multi-channel fast Fourier transform analyzer (B&K PULSE). To collect and prepare the experimental data, two microphones are located at the inlet and outlet of the silencer and spectral densities of signals are measured. The dimensions of the air suction silencer are shown in Fig. 3. The air filter and perforate holes are shown in Fig. 4, in which the hole diameter of the perforated pipes is 6 mm, the thickness 0.4 mm and the porosity 56 percent. The perforate pipes are made of galvanized steel.

4.2. Comparison of numerical analysis and experimental results

We took an air suction silencer, relatively simple three-dimensional acoustic system, as a sample acoustic system to explain and verify our method. Pre-measurements of TL of the silencer were carried out for the two cases with only the perforated tubes inserted and both the perforated tubes and filter inserted. As found in Fig. 9 presenting the measured TL's, the filter has little role in the acoustic attenuation of the silencer, as expected. Upon this finding, we excluded the filter in our study for the convenience.

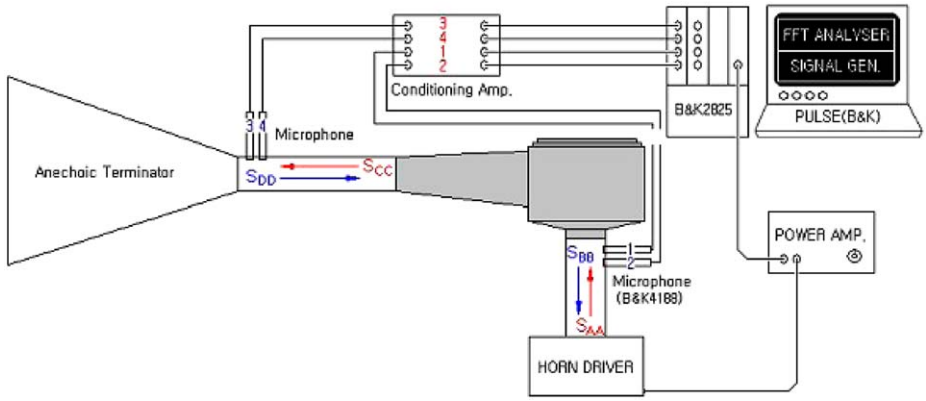

Fig. 8. Experimental setup.

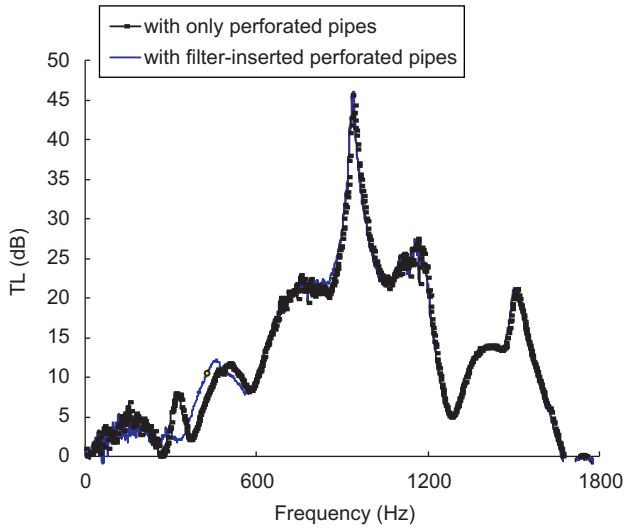

Fig. 9. Transmission losses from experiments: with only perforated pipes and with filter-inserted perforated pipes.

After all two case tests had been carried out, one case where the perforated filter guide pipes in the expansion chamber is removed and the other case where the inner and outer perforated guide pipe are installed. The air suction silencer without the guide pipes is modeled as shown in Fig. 2.

According to Fig. 3, the dimension of the silencer has the length of 510 mm, the height of 134 mm and the diameter of 225 mm. The BEM element size was decided so as to locate four or five elements within the shortest wavelength determined by the highest analysis target frequency. The frequency range of 20–2000 Hz was tested and accordingly the mean element size was taken as 34 mm. The element number of first sub-domain is 338, second sub-domain 384, third sub-domain 402 and fourth sub-domain 175, respectively.

It is shown in Fig. 10 that the numerical analysis of the silencer without the guide pipes predicts reasonably well the experimental one. And also in the case of the silencer with the perforated guide pipes, the numerical analysis approximates reasonably the experimental result, as shown in Fig. 11. But there are still somewhat large discrepancies between the BEM prediction and measurement. The discrepancies may be attributed to the fact that Eq. (16) for the acoustic impedance of the perforate was developed for low porosity (around 4.5 percent), while the porosity of perforated pipes is high (56 percent) in the present paper. Therefore, it is necessary to develop an accurate expression for the acoustic impedance of the perforate with higher porosity in the future.

These two experiments show that the developed method can be used practically to estimate the sound transmission characteristics of three-dimensional complicated silencers with perforated and/or non-perforated internal acoustic structures.

5. Conclusions

This paper proposes a practical numerical method based on multi-domain BEM data to calculate the transmission loss of three-dimensional complicated silencers. In the method, system graph approach is utilized for systematic and efficient

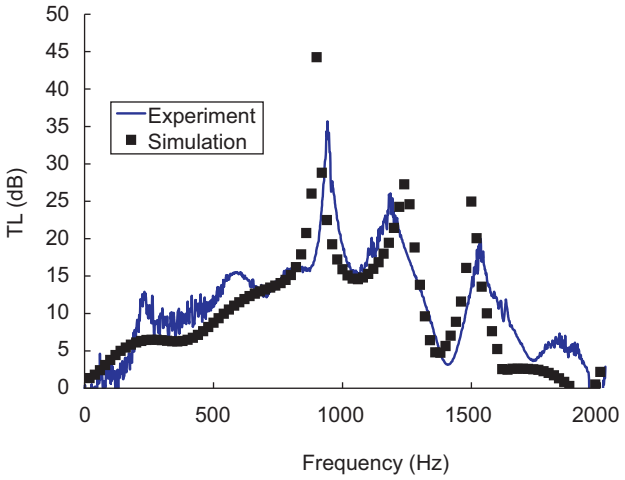

Fig. 10. Transmission losses without perforated guide pipes.

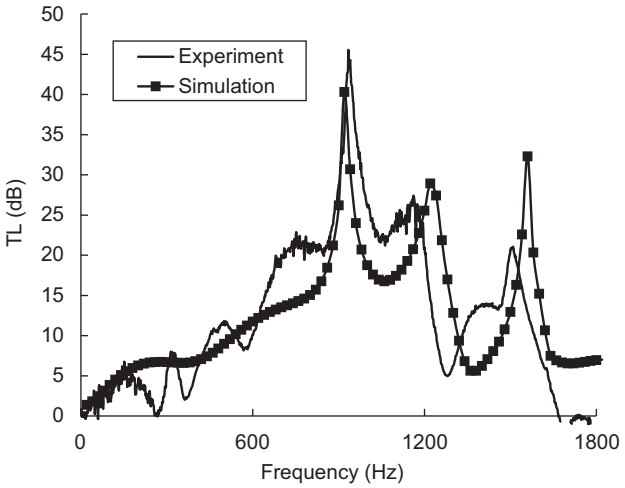

Fig. 11. Transmission losses with perforated guide pipes.

formulation of the overall acoustic system equation for the whole acoustic structure. Only the sound pressures on the sub-domain boundaries are taken as unknowns in the equations, of which the solutions are used later to compute the TL of the silencer.

The developed method can be applied extensively to the acoustic analysis and design of three-dimensional complicated silencers, which have perforated, non-perforated internal acoustic structures and absorbent materials. To confirm the performance of the proposed method, numerically analyzed and experimentally measured transmission losses for an air suction silencer were compared.

References

[1] D.A. Bies, C.H. Hansen, *Engineering Noise Control*, Unwin Hyman, London, 1988.
[2] H.D. Ju, S.B. Lee, W.B. Jeong, B.H. Lee, Design of an acoustic enclosure with duct silencers for the heavy duty diesel engine generator set, *Applied Acoustics* 65 (2004) 441–455.
[3] M.L. Munjal, *Acoustics of Ducts and Mufflers*, Wiley, New York, 1987.
[4] T. Tanaka, T. Fujikawa, A method for the analytical prediction of insertion loss of a two-dimensional muffler model based on the transfer matrix derived from the boundary element method, *Journal of Vibration, Acoustics, Stress and Reliability in Design* 107 (1985) 86–91.
[5] C.Y.R. Cheng, A.F. Seybert, A multi-domain boundary element solution for silencer and muffler performance prediction, *Journal of Sound and Vibration* 151 (1) (1991) 119–129.
[6] Z. Ji, Q. Ma, Z. Zhang, Application of the boundary element method to predicting acoustic performance of expansion chamber mufflers with mean flow, *Journal of Sound and Vibration* 173 (1) (1994) 57–71.
[7] H.D. Ju, S.B. Lee, Multi-domain structural-acoustic coupling analysis using the finite element and boundary element techniques, *Journal of Mechanical Science and Technology* 15 (2001) 555–561.

[8] A.F. Seybert, C.Y.R. Cheng, Application of the boundary element method to acoustic cavity response and muffler analysis, *Journal of Vibration, Acoustics, Stress, and Reliability in Design* 109 (1987) 15–21.
[9] T.W. Wu, P. Zhang, C.Y.R. Cheng, Boundary element analysis of mufflers with an improved method for deriving the four-pole parameters, *Journal of Sound and Vibration* 217 (4) (1998) 767–779.
[10] G. Lou, T.W. Wu, Impedance matrix synthesis for multiply connected exhaust network systems using the direct mixed-body BEM, *Journal of Sound and Vibration* 238 (2) (2000) 351–362.
[11] G. Lou, T.W. Wu, C.Y.R. Cheng, Boundary element analysis of packed silencers with a substructuring technique, *Engineering Analysis with Boundary Elements* 27 (2003) 643–653.
[12] A. Selamet, I.J. Lee, N.T. Huff, Acoustic attenuation of hybrid silencers, *Journal of Sound and Vibration* 262 (3) (2003) 509–527.
[13] Z.L. Ji, Boundary element analysis of a straight-through hybrid silencer, *Journal of Sound and Vibration* 292 (1–2) (2006) 415–423.
[14] H.D. Ju, S.B. Lee, Transmission loss estimation of three dimensional silencers with perforated internal structures using multi-domain BEM, *Journal of Mechanical Science and Technology* 19 (2005) 1568–1575.
[15] H.R. Martens, D.R. Allen, *Introduction to Systems Theory*, Charles E. Merrill Publishing Company, Columbus, Ohio, 1969.
[16] R.D. Ciskowski, C.A. Brebbia, *Boundary Element Methods in Acoustics*, Computational Mechanics Publications, Southampton, 1991.
[17] Z.L. Ji, A. Selamet, Boundary element analysis of a three-pass perforated duct mufflers, *Noise Control Engineering Journal* 48 (5) (2000) 151–156.
[18] A.F. Seybert, F. Ross, Experimental determination of acoustic properties using a two-microphone random excitation technique, *Journal of the Acoustical Society of America* 61 (1977) 1362–1370.